

## Current Topics

---

### On the Myosin Catalysis of ATP Hydrolysis<sup>†</sup>

Hirofumi Onishi,<sup>\*,‡</sup> Naoki Mochizuki,<sup>‡</sup> and Manuel F. Morales<sup>§</sup>

*Department of Structural Analysis, National Cardiovascular Center Research Institute, Fujishiro-dai, Suita, Osaka 565-8565, Japan, and University of the Pacific, San Francisco, California 94115 USA*

*Received January 6, 2004; Revised Manuscript Received February 3, 2004*

**ABSTRACT:** Myosin is an ATP-hydrolyzing motor that is critical in muscle contraction. It is well established that in the hydrolysis that it catalyzes a water molecule attacks the  $\gamma$ -phosphate of an ATP bound to its active site, but the details of these events have remained obscure. This is mainly because crystallographic search has not located an obvious catalytic base near the vulnerable phosphate. Here we suggest a means whereby this dilemma is probably overcome. It has been shown [Fisher, A. J., et al. (1995) *Biochemistry* 34, 8960–8972; Smith, C. A., and Rayment, I. (1996) *Biochemistry* 35, 5404–5417] that in an early event, Arg-247 and Glu-470 come together into a “salt-bridge”. We suggest that in doing so they also position and orient two contiguous water molecules; one of these becomes the lytic water, perfectly poised to attack the bound  $\gamma$ -phosphorus. Its hydroxyl moiety attacks the phosphorus, and the resulting proton transfers to the second water, converting it into a hydronium ion (as is experimentally observed). It is shown in this article how these central events of the catalysis are consistent with the behavior of several residues of the neighboring region.

Myosin is the key enzyme in transducing the free energy of ATP hydrolysis into the directed movements of adjoining actin filaments, so it is central in “muscle contraction”. The aim of this article is to suggest what parts of myosin execute catalysis, and how such catalysis proceeds.<sup>1</sup> The “story” we develop arises in part from our mutational studies (1–3) but is heavily dependent on the crystallographic studies of Rayment et al. (4–6), and more recently those of Cohen et

al. (7, 8). The importance of explaining myosin catalysis has been evident. But as Rayment (5) has pointed out, progress has been thwarted because there appears to be no (necessary) proton acceptor within 5.5 Å of the vulnerable P–O linkage of bound ATP; nevertheless, we have paid attention to Rayment’s note of a “water network” (6). Also, we have learned much from analogizing with the G-protein system that catalyzes the hydrolysis of GTP (9–11). Our program here is to present a reasonable hypothesis about events that

---

<sup>†</sup> This work was supported by Grant-in-Aids for Scientific Research and by Special Coordination Funds for Promoting Science and Technology from the Ministry of Education, Culture, Sports, Science, and Technology (to H.O. and N.M.) and by Grant MCB 9603670 from the National Science Foundation (to M.F.M.). A condensed version of this study was presented at the annual meeting of the American Biophysical Society held in San Antonio, Texas on March 2, 2003 (*Biophys. J.* 84, No. 2, Part 2 of 2, 3a, 2003).

\* Address correspondence to this author: Tel: +81-6-6833-5012. Fax: +81-6-6872-8092. E-mail: honishi@ri.ncvc.go.jp.

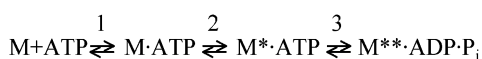
<sup>‡</sup> National Cardiovascular Center Research Institute.

<sup>§</sup> University of the Pacific.

---

<sup>1</sup> In muscle contraction, a second protein, actin, is an essential partner, which, in addition to substrate, interacts with myosin. However, myosin alone is able to catalyze ATPase, and it is to this simplified system (myosin + substrate + ions + water) that this article refers. When actin is also present, the rates at which myosin conducts various processes that comprise its catalysis are very different. It is logically possible that the qualitative nature of its catalysis inside its catalytic cleft is then also different; however, because even in the presence of actin, hydrolysis occurs after myosin has released from actin, and myosin rebinds actin at its M\*\*\*ADP·P<sub>i</sub> state, such a circumstance seems very unlikely, but should be kept in mind.

Scheme 1



lead up to positioning the “lytic” water destined to attack the  $\gamma$ -phosphate moiety of myosin-bound ATP—along the way showing how nature probably supplies the “missing” proton acceptor.

**Informational Background.** We are especially concerned with the early events of myosin catalysis, beginning with what happens in the myosin molecule just after a nucleotide, such as ATP, binds to its “active site”, and is being prepared for hydrolysis. In terms of the Trentham-Bagshaw kinetic scheme (12, 13), these early events are described by Scheme 1 where M and  $\text{P}_i$  are myosin and inorganic phosphate, respectively, and \* and \*\* indicate conformers distinguishable by absorbance (14) or fluorescence (15). Recent studies have identified the residue bearing the optical sensor as Trp-512<sup>2</sup> (16–22).

Rayment and his successors have begun to reconstruct the transformations of the hydrolyzing myosin-nucleotide system by successively taking crystallographic “snapshots” of the system in the order in which they think the real transformations occur (5, 6, 23). Of course, each snapshot has to be static, made by using, for example, a stable non-hydrolyzing intermediate thought to be analogous to the real intermediate. By such an approach, they have made intelligent guesses about the highly resolved structures in a succession of myosin states.

Building on the crystallography, we have, in parallel, tried to study the real system as it passes rapidly through the same transformations, attempting, by kinetic measurements, to sample *all* the states—among these the ones resolved in the snapshots. In applying our approach, however, we can use site-directed mutation, i.e., examine in the same way *various* systems, differing from each other in structure only at *one* residue position.<sup>3</sup> Comparison of the behavior of such systems, say the normal (“wild type”) and a particular mutated system, often suggests something about the role of that residue in the normal system. What follows is a comprehensive hypothesis of how myosin catalysis works, based on our synthesis of crystallographic and conventional biochemical knowledge.

A graphic impression of how events of our interest begin is given by Figure 1, which also illustrates the “successive snapshot” logic used by crystallographers. It is thought that stable systems of ATP analogues,  $\text{ADP} \cdot \text{BeF}_x$  and  $\text{ADP} \cdot \text{VO}_4^-$ , respectively, are legitimate models from which to infer the behavior of molecules containing authentic ATP in the

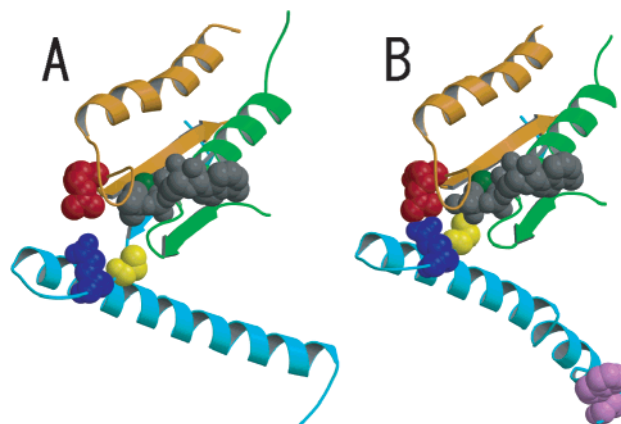


FIGURE 1: Ribbon representation of the nucleotide-binding pocket of the open (A) and closed (B) forms of myosin. Crystal structures of *Dictyostelium* myosin motor domain complexed with  $\text{MgADP} \cdot \text{BeF}_x$  (ref 5: PDB entry 1MMD) and  $\text{MgADP} \cdot \text{VO}_4^-$  (ref 6: PDB entry 1VOM) are adopted for the open and closed forms, respectively. Backbone atoms of the sequences of residues 167–203 (P-loop), 218–258 (Switch I), and 457–513 (Switch II) of the heavy chain are colored green, orange, and light blue, respectively. Bound nucleotides,  $\text{Mg}^{2+}$ , Arg-247, Gly-468, Glu-470, and Trp-512 are shown as space-filled balls in gray, dark green, red, yellow, blue, and violet, respectively. Note that a salt-bridge is formed between residues Arg-247 and Glu-470 in the closed form. Also note that in this form, Gly-468 is in contact with the  $\gamma$ -phosphate moiety of the bound nucleotide. The nucleotide-responsive tryptophan residue (Trp-512) is connected with the Switch II loop by a long  $\alpha$ -helix.

prehydrolytic and transition states, and in the presence of other participants in the system (5, 6). With these provisos, we can portray what probably happens during a process in which the cleft region of myosin, having bound ATP, transits from one state to another. Understood is that the system as a whole suffers an accompanying free energy decrement. We cannot express such a change in structural detail, but a very notable item is that, in the process, two flexible loop residues—Arg-247 and Glu-470—initially remote from each other, come into a “salt-bridge”. Seemingly as a result, the binding cleft closes over the bound substrate, and immediately, the distant Trp-512 responds by increasing its fluorescence. (Note that cleft and Trp-512 are connected by a long but rigid helix. It is for this reason that enhanced fluorescence is taken to signal cleft closing). Thereafter, the  $\gamma$ -phosphate of the bound nucleotide is in some way prepared for its catalyzed hydrolysis.

Early on, Glu-470 interested us (1) because of its suspicious location near the  $\gamma$ -phosphate of the bound nucleotide, and even more later after Rayment (5, 6) discovered the salt-bridge formation. To study the situation more deeply, we prepared and analyzed several mutant systems (2, 3). In some, Arg-247 was replaced by Ala or Glu, and in some, Glu-470 was replaced by Ala or Arg. In one, the assignments of Arg and Glu were reversed to Glu and Arg. To track the systems in time (step 1 in Scheme 1), we used mantATP<sup>4</sup> instead of ATP, and for step 2, we used the equivalent fluorescence from Trp-512. In each case, we assessed the ability to hydrolyze nucleotide triphosphate by its production of inorganic phosphate (step 3). From these experiments, we drew many important conclusions (2, 3), for example, that

<sup>2</sup> Although the amino acid sequence of a protein is different in various organisms (or in different major tissues of the same organism), well-established homologies permit interspecific translation from one species to another. Throughout, we use the sequence numeration appropriate for smooth muscle myosin, as extracted from chicken gizzard. We note that Lys-183, Thr-184, Asn-242, Asn-244, Ser-245, Ser-246, Arg-247, Asp-465, Ile-466, Ala-467, Gly-468, Glu-470, and Trp-512 correspond to *Dictyostelium discoideum* Lys-185, Thr-186, Asn-233, Asn-235, Ser-236, Ser-237, Arg-238, Asp-454, Ile-455, Ser-456, Gly-457, Glu-459, and Trp-501.

<sup>3</sup> The myosin properties of present concern all exist in the truncated, proteolytically obtainable, two-headed structure known as “heavy meromyosin”, and used in our experiments, so we do not distinguish between our structure and truly intact myosin, for which “M” is intended to stand.

<sup>4</sup> Abbreviation: mantATP, 2'(3')-O-(N-methylanthraniloyl) adenosine 5'-triphosphate.

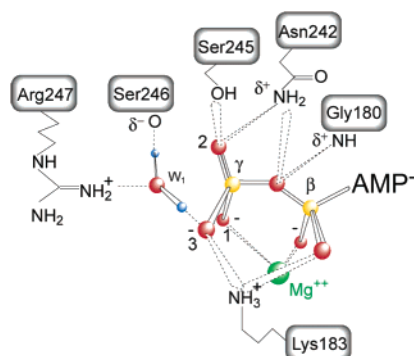


FIGURE 2: The structure of the prehydrolysis state ( $M\cdot ATP$ ). The  $\gamma$ -phosphate of ATP is in a tetrahedral arrangement with its four oxygen atoms. A water molecule involved in hydrogen bonding with the  $\gamma$ -phosphate is denoted as  $w_1$ . We assume that this water is HOH1181 in the Fisher et al. structure (ref 5, 1MMD). The  $\beta$ - and  $\gamma$ -phosphate groups of ATP,  $Mg^{2+}$ , and the water molecule are shown in ball-and-stick form. Covalent bonds are shown as solid lines and hydrogen bonds and ionic interactions in dashed lines. Phosphorus, oxygen, hydrogen, and magnesium are depicted in yellow, red, blue, and green, respectively.

probably the electrical force between Arg-247 and the bound triphosphate moiety helps to close the cleft and to signal Trp-512. On the other hand, we felt that the close correlation between the presence of Glu at position 470 and hydrolysis probably meant that that particular residue had a role in catalysis. From the foregoing beginnings, we now commence to put together our hypothesis in the sequence that we suppose will be easiest to verify.

**The Prehydrolytic State.** Key features of relevant  $M\cdot ATP$  structure, i.e., of the situation at the active site, are in Figure 2 (abstracted from a Rayment snapshot of bound  $MgADP\cdot BeF_3$ ). Three oxygen atoms (1, 2, and 3) of the  $\gamma$ -phosphate group are bound and oriented by bound  $Mg^{2+}$ , the side chains of Asn-242 ( $N_{\delta 2}$ ) and Ser-245 ( $O_\gamma$ ) of Switch I, and Lys-183 of the P-loop, respectively. A single molecule of water,  $w_1$ , is attached to the guanidino group of Arg-247 ( $N_{\eta 1}$ ), which interacts with a main chain carbonyl oxygen of Ser-246 of Switch I, and is attached to oxygen (3) of the  $\gamma$ -phosphate moiety of the bound nucleotide. (Note: The orientation of  $w_1$  is similar to that of a water molecule at the active site of transducin  $G_\alpha$  complexed with  $GTP\gamma S$  that mimics the ground state of bound  $GTP$  (11)). Because earlier we found a good correlation between the presence of Arg at position 247 and the rate of substrate binding to the active site (3), we speculated above that Arg-247 indirectly, perhaps by its electrical force, interacts with the  $\gamma$ -phosphate moiety via  $w_1$ , and so for this reason this positive residue is important for binding substrate to the active site. In this ground state, however,  $w_1$  does not yet have the position to act (see below).

**Closure of the Nucleotide-Binding Cleft.** Figure 3 depicts diagrammatically how we think this cleft closes: (A) repeats the same stage depicted in Figure 2; (B) is an intermediate stage; and (C) is the final stage. Comparison of the three stages implies that on closure there is a big structural change in Switch II (in light blue), but none in Switch I (in black).

In Figure 3A the cleft is still open, so the Switch II residues, excepting Asp-465, do not interact with either the bound nucleotide or the bound  $Mg^{2+}$  at this stage.  $Mg^{2+}$  is very important in closure because of its location in the cleft. It is central in chelating the  $\beta$ - and  $\gamma$ -phosphates of the

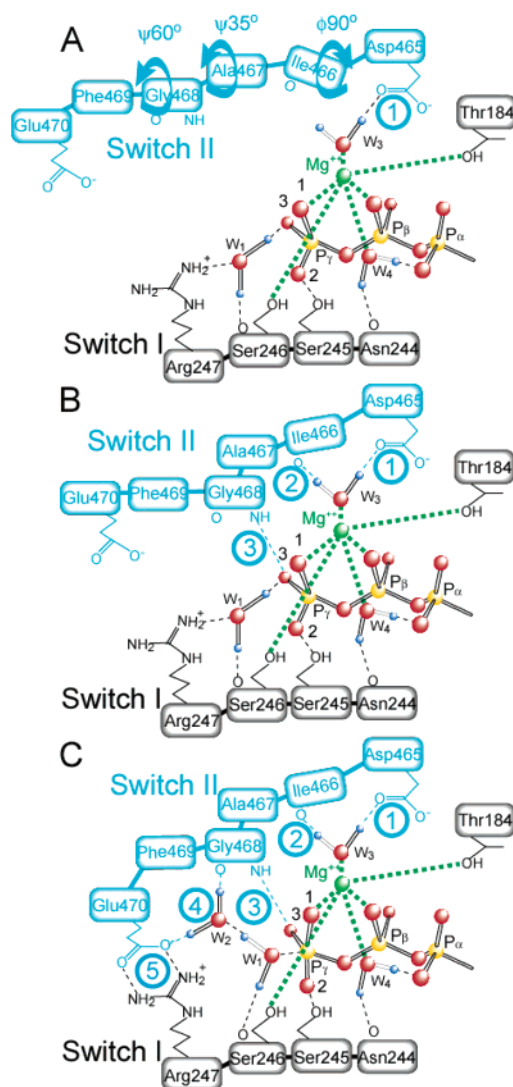


FIGURE 3: The closing process of the nucleotide-binding cleft. A series of diagrams show the disposition in space of the Switch II strand (colored light blue) at three different times after nucleotide binds to the active site: A, the early stage; B, the intermediate stage; and C, the final stage. In the diagrams, we also show how the  $\gamma$ -phosphate moieties of bound nucleotide are associated with the strand. We assume that  $w_1$  in A is HOH1181 in the Fisher et al. structure (ref 5, 1MMD) and that  $w_1$  and  $w_2$  in C take the place of the terminal oxygen atom of the vanadate moiety and that of HOH697, respectively, in the Smith and Rayment structure (ref 6, 1VOM). Three curved arrows show the general direction in which relevant Ramachandran angles change in the transition from the A to the B state (the angle and the amount of its change are given). The progressive attachments of the Switch II strand occur in the sequence given by the circled numeral. Covalent bonds are shown as solid lines and hydrogen bonds and ionic interactions in dashed lines. Coordinated interactions with the  $Mg^{2+}$  of bound nucleotide are shown as green, thick dashed lines. Phosphorus, oxygen, hydrogen, and magnesium are depicted in yellow, red, blue, and green, respectively.

nucleotide, and in its coordination sphere are six ligands in octahedral geometry. Also,  $Mg^{2+}$  is connected with both the P-loop via  $O_{\gamma 1}$  of Thr-184 and Switch I via  $O_\gamma$  of Ser-246. Two water molecules are coordinated to  $Mg^{2+}$ . One,  $w_4$ , interacts with the main chain carbonyl oxygen of Asn-244, and also bonds to an oxygen atom of the  $\alpha$ -phosphate group. One of the hydrogen atoms of another water molecule,  $w_3$ , interacts with the side chain of Asp-465 ( $O_{\delta 2}$ ). This fact,

and his own work on mutations, led Sutoh to suggest that Asp-465 is important in nucleotide binding (24). We propose that  $w_1$  retains its attachment to Switch I, and that, by virtue of the intervention of  $w_3$  (which inserts between the  $Mg^{2+}$  associated with Switch I via the bound nucleotide and a carboxyl oxygen atom of Asp-465 of Switch II), the closing of the cleft is initiated. The three curved arrows in Figure 3A indicate the direction in which the relative Ramachandran angles change in the transition between states. When Ile-466 rotates (permitted by the flexibility of the Switch II loop) in such a way that its Ramachandran angle  $\phi$  increases by  $90^\circ$ , the oxygen atom of its main chain carbonyl group moves toward  $w_3$ , and can now form a bond with the other hydrogen atom of the  $w_3$ . Accompanying changes in the  $\phi$  angles of Ala-467 and Gly-468 (see Figure 3A) create an interaction between the main chain amide hydrogen of Gly-468 and the  $\gamma$ -phosphate moiety of the bound nucleotide. (See Figure 3B.) At this stage,  $w_2$  first appears in the crystallographic image of the phosphate pocket of the enzyme. It is hydrogen-bonded to the main chain carbonyl oxygen of Gly-468, and to one of the two oxygen atoms of the carboxyl group of Glu-470 ( $O_{e1}$ ). See Figure 3C. As earlier noted, Trp-512 is remotely connected to Switch II in the active site; it is at this stage that Trp-512 is "informed" and increases its fluorescence. (See Scheme 1.)

Although, strictly speaking, observations of the sort we are citing cannot be put in cause-to-effect relations, cleft closure is closely correlated in time with at least two other important events. One is that, with closure, force appears to be transmitted via the long  $\alpha$ -helix, across the so-called "converter" region, to what appears to be the myosin "lever arm" (7). It is known that in a myosin "motor", the mechanical working (power) stroke is time-correlated with the phosphate release step that follows hydrolysis (Figure 4). Also, Sutoh et al. (25) showed that a large angle change of the lever arm occurring during  $M \cdot ATP \rightarrow M^* \cdot ATP$  is necessary for the reverse of the power stroke motion. Other events also associated with closure (to be discussed later) are a hydrogen-bond interaction between Gly-468 and an oxygen atom of the  $\gamma$ -phosphate, and the formation of the salt-bridge between side chains of Arg-247 and Glu-470—all crucial for setting up catalysis.

**The Transition State for Hydrolysis.** In the snapshot taken to represent the situation at the time of hydrolysis ( $MgADP \cdot VO_4^-$  bound to the active site), the cleft is closed and there are two molecules of water bound in the  $\gamma$ -phosphate pocket (6). We suppose (Figure 3C) that movement of Glu-470 permits its bridging toward the guanidino group of Arg-247, which then releases its water,  $w_1$ , destined to become the "lytic" water. One of the hydrogen atoms of this water, initially bonded to an oxygen atom of the  $\gamma$ -phosphate group, then interacts with the oxygen atom of a new, intruding water,  $w_2$ . The other hydrogen atom remains bonded to the main chain carbonyl oxygen of Ser-246. A result of making this critical conjecture is that then  $w_1$  ends up partially positioned and oriented to carry out its attack on the  $\gamma$ -phosphorus (cf., the analogous location of the lytic water in the active site of transition-state transducin  $G_\alpha$  (11)). Even at this stage, however, our conjecture already responds to certain requirements. It provides explanations of why two water molecules are seen in the snapshot of the transition state (6), why the ability of a system to catalyze hydrolysis

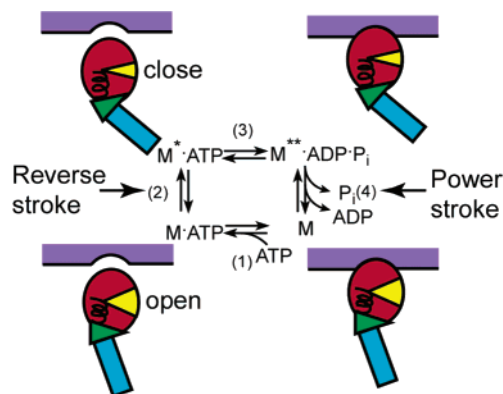


FIGURE 4: Some important transformations during the ATPase cycle. Chemically, myosin (M) binds to ATP, hydrolyzes it to ADP· $P_i$ , and releases the products. To function in muscle contraction myosin must undergo (a) a conformational change that switches between actin-binding and actin-release states, and (b) a conformational change that swings the lever arm for contraction ("power stroke"). Presumably, a sequence that must occur in muscle is (1) the conformational change that allows release from actin, (2) the conformational change that reverse swings the lever arm, (3) the conformational change to the actin-binding state, and (4) the conformational change that swings the lever arm in the power stroke. In this article, however, we are only concerned with conformational change (2) and the following hydrolysis. As the product release from  $M^* \cdot ADP \cdot P_i$ , at which the power stroke occurs, is greatly accelerated by actin, it seems reasonable to assume that the transition to the actin-binding state occurs in the state  $M^* \cdot ADP \cdot P_i$ . However, the conformational change during this transition is not well clarified yet. The reverse and power strokes occur at the stages indicated. This figure also denotes the relationship of myosin to actin (free or bound). The motor domain is depicted in red, the converter in green, the lever arm in blue, the nucleotide-binding cleft in yellow, and the actin filament in violet. A long, conserved  $\alpha$ -helix that connects between the binding cleft and the converter is shown as a spiral in the motor domain.

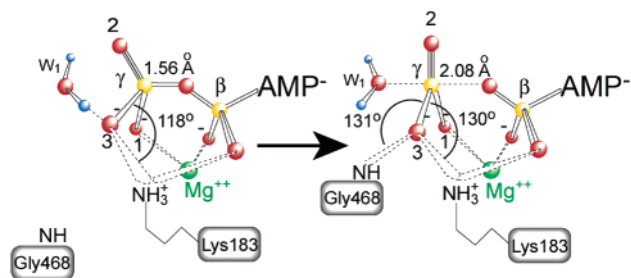


FIGURE 5: A mechanism for the change of the  $\gamma$ -phosphate configuration. The left and right diagrams represent the tetrahedral and the trigonal bipyramidal structures, respectively. The  $\beta$ - and  $\gamma$ -phosphate of ATP, the  $Mg^{2+}$ , and a water molecule are shown as a ball-and-stick model. Oxygen atoms interacted with  $Mg^{2+}$ , Ser-245, and Lys-183 are denoted as 1, 2, and 3, respectively. Angles of  $P_\gamma-O-N_{\text{Lys-183}}$  and  $P_\gamma-O-N_{\text{main chain of Gly-468}}$ , and the distance between the  $\gamma$ -phosphorus and the  $\beta$ - $\gamma$  bridging oxygen are given from the crystal structures (1MMD for the left diagram and 1VOM for the right diagram).

is tightly correlated to the presence of Glu at position 470 (3), and why the Rayment (6) surmise of a functional role for a "water network" was prophetic.

Although already partly positioned by  $w_2$  and Ser-246, we believe that  $w_1$  is not yet at its final attack position and that its final positioning results from the shift of the  $\gamma$ -phosphate structure from its tetrahedral to its trigonal bipyramidal configuration. As already stated, we cannot assign cause-to-effect relationships, but do think that the final positioning

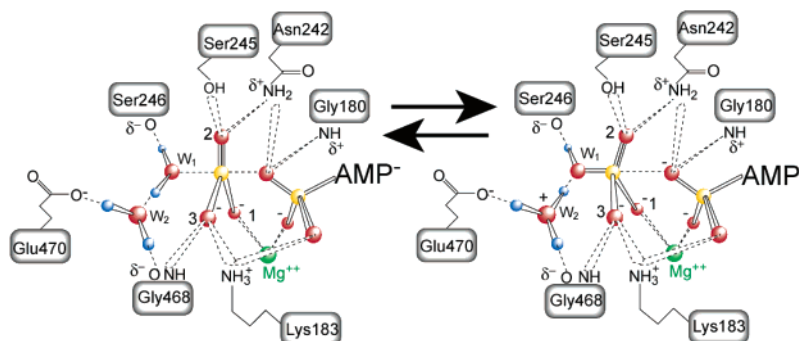


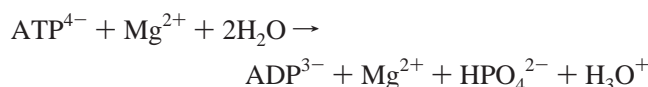
FIGURE 6: The transfer of a proton from  $w_1$  to  $w_2$  and the production of  $P_i$  and  $H_3O^+$ . The left and right diagrams represent the structures for the transition and posthydrolysis states, respectively.  $\delta^+$  and  $\delta^-$  indicate positive and negative charges, respectively, which are induced by the resonance structures of the peptide bond. Covalent bonds are shown as filled lines, and hydrogen bonds and ionic interactions in dashed lines. The  $\beta$ - and  $\gamma$ -phosphates of ATP,  $Mg^{2+}$ , and two water molecules are shown as a ball-and-stick model.

ends a series of identifiable events. It will be recalled that Gly-468 is the only residue whose interaction with the  $\gamma$ -phosphate is induced by the cleft closure. One of possible speculations about the conformational change of the  $\gamma$ -phosphate now follows. As is well-known, the normal angle of separation between two oxygen bonds is about  $105^\circ$ . In the prehydrolysis state ( $MgADP \cdot BeF_x$  bound to the active site), this angle in  $P_\gamma-O-N_\xi$  of Lys-183 is  $118^\circ$  (quasi normal) (left, Figure 5). So, we suggest that when the cleft is open (Gly-468 is away from the  $\gamma$ -phosphate), the tetrahedral is preferred over the trigonal bipyramidal configuration. In the transition state for hydrolysis ( $MgADP \cdot VO_4^-$  bound to the active site), the  $P_\gamma-O-N_\xi$  angle becomes significantly larger, viz.,  $130^\circ$  (right, Figure 5). In contrast, the  $P_\beta-O-N_\xi$  angle of the same Lys-183 remains essentially constant during the same transit ( $111^\circ$  vs  $114^\circ$ ). As cited earlier (Figure 3B), the main chain amide nitrogen ( $N_{main\ chain}$ ) of Gly-468 creates an interaction with oxygen (3) of the  $\gamma$ -phosphate during the transit to the transition state. The  $P_\gamma-O-N_{main\ chain}$  angle of Gly-468 was  $131^\circ$ , essentially the same as the new  $P_\gamma-O-N_\xi$  angle of Lys-183. This circumstance suggests a reason why interaction of Gly-468 with the  $\gamma$ -phosphate energetically disposes  $\gamma$ -phosphate to leave from the bridging oxygen between  $\beta$ - and  $\gamma$ -phosphates, and at the same time changes its configuration. If this speculation is granted, several observations are conveniently explained, e.g., why the trigonal bipyramidal configuration is observed only in structures in which the cleft is closed (5, 6), why the K183A<sup>5</sup> system can catalyze hydrolysis even though Lys-183 is involved in the catalysis (unpublished observations), and why, as earlier observed (1), the G468A system exhibits neither steady-state ATPase nor an initial phosphate burst.

**“Two-Water” Hypothesis of How Myosin Catalyzes ATPase.** As described in the foregoing section,  $w_1$  is now oriented to carry out its attack on the  $\gamma$ -phosphate, and, on the other side, the  $\gamma$ -phosphate is readied for the attack from  $w_1$  by changing its configuration into a trigonal bipyramidal. Now, we deal with the question of how hydrolysis proceeds to produce  $P_i$  and ADP. No crystal structure of the post-hydrolysis state is available, but we can make some guesses about the passage from the transition state to the post-

hydrolysis state. Our proposal resembles catalysis by the GTPase system. Coleman and Sprang (9) have reviewed the latter system, explaining the participation of highly conserved Gln and Arg (in  $G_{i\alpha}$ , Gln-204 and Arg-178). In our hypothesis, Glu-470– $w_2$ –Gly-468 and Asn-242, respectively, play analogous roles. The essential transformations are depicted in Figure 6. On the left is the transition state, and on the right is a state resulting from hydrolysis. When the  $\gamma$ -phosphate approaches,  $w_1$  splits, the resulting hydroxyl moiety attacks the  $\gamma$ -phosphate (to form  $P_i$ ), and the resulting proton transfers to  $w_2$  (to form  $H_3O^+$ ). The positive charge developed at  $w_2$  is stabilized by both the carboxyl group of Glu-470 and the main chain carbonyl oxygen of Gly-468, both of which are negatively charged (denoted as  $\delta^-$ ). After  $P_i$  leaves, the terminal oxygen atom of the  $\beta$ -phosphate group of ADP is also ionized. This negative charge is neutralized by the side chain of Asn-242 ( $N_{\delta 2}$ ) and the main chain amide of Gly-180, both of which are positively charged (denoted as  $\delta^+$ ). This model is consistent with crystallographic observations suggesting that Asn-242 and Gly-180 both interact with the bridging oxygen atom of the  $\beta$ -phosphate (5, 6), and also harmonizes with our results that in the N242A system both steps of  $M^{*} \cdot ADP \cdot P_i \rightarrow M^{*} \cdot ADP + P_i$  and the displacement of  $M^{*} \cdot ADP$  are 10 times faster than in the wild-type system (unpublished observations). Our proposal thus resolves the long-standing conundrum about how catalysis seems to be carried out absent an obvious hydrogen acceptor.

Earlier kinetic studies have shown that per mole of ATP hydrolyzed at pH 8.0, one mole of protons is produced, at the rate limitation corresponding to  $P_i$  release (12, 13, 26). Because protons in water exist as hydronium ions, the appropriate chemical equation is



It seems important that our hypothesis accounts stoichiometrically for each of the chemical species in this equation. These kinetic studies have also shown that for the enzyme-bound system, the equilibrium constant for hydrolysis is near to unity (12, 13, 26), so it is plausible to assume that at this stage there is a rapid interconversion between similarly weighted structures and thus to account for how experiments in  $H_2^{18}O$  yield  $^{18}O$ -labeling of more than one per mole (27–29). This feature of the catalysis may or may not bear on

<sup>5</sup> A mutant is represented by a one-letter expression of the original amino acid residue prior to its sequence number, and that of the mutated residue following to its number, i.e., R183A, G468A, and N242A.

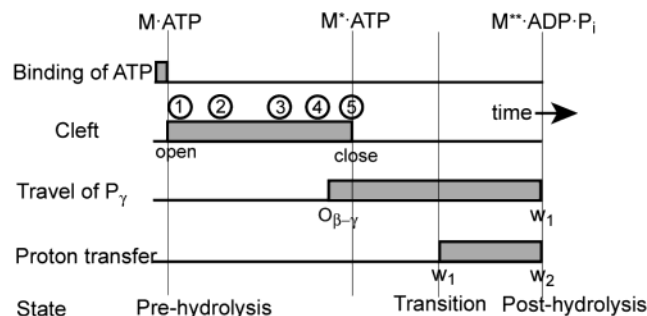


FIGURE 7: A chronological sequence of events during ATP hydrolysis. The period of each event is shown as a gray zone. 1, 2, 3, 4, and 5 represent coordination of Asp-465 to  $Mg^{2+}$  via  $w_3$ , Ramachandran angle changes at Ile-466, Ala-467, and Gly-468, hydrogen-bonding of Gly-468 to an oxygen of the  $\gamma$ -phosphate, trapping of  $w_2$  between Gly-468 and Glu-470, and salt-bridge formation between Glu-470 and Arg-247, respectively.

how excess labeling of  $P_i$  is interpreted. It is conceivable that although the crystallographically observed number of water molecules inside of the cleft is small, the actual number of water molecules in free exchange with the cleft may be large. In that case, the usual mechanism (interconversion and random labeling) can be invoked.

The name that we use for our proposal stems from our thinking that, in essence, two contiguous water molecules are involved in catalysis, i.e., one becomes the lytic water and the other is the proton acceptor. However, as we have attempted to show, this simplification is embedded in a program of complicated, well-coordinated processes that together constitute “myosin catalysis”. Some tracks in time are shown in Figure 7. If we commence a myosin cycle with the binding of ATP to an empty active site (forming of  $M \cdot ATP$ ), we must think of the cleft closing, which is followed by two processes. One is hydrogen-bonding of the main chain nitrogen atom of Gly-468 to an oxygen atom of the  $\gamma$ -phosphate (denoted as 3 in Figure 7), which affects the choice of the  $\gamma$ -phosphate configuration. As a result, the  $\gamma$ -phosphorus begins its long travel from the  $\beta$ - $\gamma$  bridging oxygen to  $w_1$ ; in other words, inversion of the  $\gamma$ -phosphate begins. Other processes following cleft closing are Arg-247 and Glu-470 forming of the salt-bridge (denoted as 5 in Figure 7), trapping of  $w_2$  by its hydrogen-bonding with both Glu-470 and Gly-468,  $w_1$  leaving from the guanidino group of Arg-247, and hydrogen-bonding between  $w_1$  and  $w_2$ . Finally, a nucleophilic attack of  $w_1$  on the  $\gamma$ -phosphate, coupled with the proton transfer from  $w_1$  to  $w_2$ , occurs to produce  $P_i$  and  $H_3O^+$ .

While plausible variants of the “two-water” idea are conceivable, as are elaborations of the role of Lys-183 (30, 31), such a variant must contend with the experimental fact that the mutated system with alanine in place of lysine still accomplishes hydrolysis. Also, any variant must explain why it is necessary to have glutamic acid at 470 to accomplish hydrolysis.

## ACKNOWLEDGMENT

We are grateful to Professor H. M. Martinez for his helpful counsel and Professors I. Rayment and D. McKay for significant improvements in our manuscript.

## REFERENCES

- Onishi, H., Morales, M. F., Kojima, S., Katoh, K., and Fujiwara, K. (1997) Functional transitions in myosin: role of highly conserved Gly and Glu residues in the active site. *Biochemistry* 36, 3767–3772.
- Onishi, H., Kojima, S., Katoh, K., Fujiwara, K., Martinez, H. M., and Morales, M. F. (1998) Functional transitions in myosin: formation of a critical salt-bridge and transmission of effect to the sensitive tryptophan. *Proc. Natl. Acad. Sci. U.S.A.* 95, 6653–6658.
- Onishi, H., Ohki, T., Mochizuki, N., and Morales, M. F. (2002) Early stages of energy transduction by myosin: roles of Arg in switch I, of Glu in switch II, and of the salt-bridge between them. *Proc. Natl. Acad. Sci. U.S.A.* 99, 15339–15344.
- Rayment, I., Rypniewski, W. R., Schmidt-Bäse, K., Smith, R., Tomchick, D. R., Benning, M. M., Winkelman, D. A., Wesenberg, G., and Holden, H. M. (1993) Three-dimensional structure of myosin subfragment-1: a molecular motor. *Science* 261, 50–58.
- Fisher, A. J., Smith, C. A., Thoden, J. B., Smith, R., Sutoh, K., Holden, H. M., and Rayment, I. (1995) X-ray structures of the myosin motor domain of *Dictyostelium discoideum* complexed with  $MgADP \cdot BeFx$  and  $MgADP \cdot AlF_4^-$ . *Biochemistry* 34, 8960–8972.
- Smith, C. A., and Rayment, I. (1996) X-ray structure of the magnesium(II)-ADP-vanadate complex of the *Dictyostelium discoideum* myosin motor domain to 1.9 Å resolution. *Biochemistry* 35, 5404–5417.
- Dominguez, R., Frey, Y., Trybus, K. M., and Cohen, C. (1998) Crystal structure of a vertebrate smooth muscle myosin motor domain and its complex with the essential light chain: visualization of the pre-power stroke state. *Cell* 94, 559–571.
- Houdusse, A., Kalabokis, V. N., Himmel, D., Szent-Györgyi, A. G., and Cohen, C. (1999) Atomic structure of scallop myosin subfragment S1 complexed with  $MgADP$ : a novel conformation of the myosin head. *Cell* 97, 459–470.
- Coleman, D. E., and Sprang, S. R. (1999) Reaction dynamics of G-protein catalyzed hydrolysis of GTP as viewed by X-ray crystallographic snapshots of  $G_{i\alpha 1}$ . *Methods Enzymol.* 308, 70–92.
- Coleman, D. E., Berghuis, A. M., Lee, E., Linder, M. E., Gilman, A. G., and Sprang, S. R. (1994) Structures of active conformations of  $G_{i\alpha 1}$  and the mechanism of GTP hydrolysis. *Science* 265, 1405–1412.
- Sondek, J., Lambright, D. G., Noel, J. P., Hamm, H. E., and Sigler, P. B. (1994) GTPase mechanism of G-proteins from the 1.7-Å crystal structure of transducin  $\alpha$ -GDP- $AlF_4^-$ . *Nature* 372, 276–279.
- Bagshaw, C. R., and Trentham, D. R. (1974) The characterization of myosin-product complexes and of product-release steps during the magnesium ion-dependent adenosine triphosphatase reaction. *Biochem. J.* 141, 331–349.
- Bagshaw, C. R., Eccleston, J. F., Eckstein, F., Goody, R. S., Gutfreund, H., and Trentham, D. R. (1974) The magnesium ion-dependent adenosine triphosphatase of myosin. Two-step processes of adenosine triphosphate association and adenosine diphosphate dissociation. *Biochem. J.* 141, 351–364.
- Morita, F. (1967) Interaction of heavy meromyosin with substrate. I. Difference in ultraviolet absorption spectrum between heavy meromyosin and its Michaelis–Menten complex. *J. Biol. Chem.* 242, 4501–4506.
- Werber, M. M., Szent-Györgyi, A. G., and Fasman, G. D. (1972) Fluorescence studies on heavy meromyosin-substrate interaction. *Biochemistry* 11, 2872–2883.
- Johnson, W. C., Jr., Bivin, D. B., Ue, K., and Morales, M. F. (1991) A search for protein structural changes accompanying the contractile interaction. *Proc. Natl. Acad. Sci. U.S.A.* 88, 9748–9750.
- Hiratsuka, T. (1992) Spatial proximity of ATP-sensitive tryptophanyl residue(s) and Cys-697 in myosin ATPase. *J. Biol. Chem.* 267, 14949–14954.
- Batra, R., and Manstein, D. J. (1999) Functional characterisation of *Dictyostelium* myosin II with conserved tryptophanyl residue 501 mutated to tyrosine. *Biol. Chem.* 380, 1017–1023.
- Yengo, C. M., Chrin, L. R., Rovner, A. S., and Berger, C. L. (2000) Tryptophan 512 is sensitive to conformational changes in the rigid relay loop of smooth muscle myosin during the  $MgATPase$  cycle. *J. Biol. Chem.* 275, 25481–25487.

20. Park, S., and Burghardt, T. P. (2002) Tyrosine mediated tryptophan ATP sensitivity in skeletal myosin. *Biochemistry* 41, 1436–1444.
21. Onishi, H., Konishi, K., Fujiwara, K., Hayakawa, K., Tanokura, M., Martinez, H. M., and Morales, M. F. (2000) On the tryptophan residue of smooth muscle myosin that responds to binding of nucleotide. *Proc. Natl. Acad. Sci. U.S.A.* 97, 11203–11208.
22. Malnasi-Csizmadia, A., Woolley, R. J., and Bagshaw, C. R. (2000) Resolution of conformational states of *Dictyostelium* myosin II motor domain using tryptophan (W501) mutants: implications for the open-closed transition identified by crystallography. *Biochemistry* 39, 16135–16146.
23. Gulick, A. M., Bauer, C. B., Thoden, J. B., and Rayment, I. (1997) X-ray structures of the MgADP, MgATP $\gamma$ S, and MgAMPPNP complexes of the *Dictyostelium discoideum* myosin motor domain. *Biochemistry* 36, 11619–11628.
24. Sasaki, N., Shimada, T., and Sutoh, K. (1998) Mutational analysis of the switch II loop of *Dictyostelium* myosin II. *J. Biol. Chem.* 273, 20334–20340.
25. Suzuki, Y., Yasunaga, T., Ohkura, R., Wakabayashi, T., and Sutoh, K. (1998) Swing of the lever arm of a myosin motor at the isomerization and phosphate-release steps. *Nature* 396, 380–383.
26. Lymn, R. W., and Taylor, E. W. (1971) Mechanism of adenosine triphosphate hydrolysis by actomyosin. *Biochemistry* 10, 4617–4624.
27. Levy, H. M., and Koshland, D. E. (1959) Mechanism of hydrolysis of adenosinetriphosphate by muscle proteins and its relation to muscular contraction. *J. Biol. Chem.* 234, 1102–1107.
28. Webb, M. R., and Trentham, D. R. (1981) The mechanism of ATP hydrolysis catalyzed by myosin and actomyosin, using rapid reaction techniques to study oxygen exchange. *J. Biol. Chem.* 256, 10910–10916.
29. Bowater, R., Zimmerman, R. W., and Webb, M. R. (1990) Kinetics of ATP and inorganic phosphate release during hydrolysis of ATP by rabbit skeletal actomyosin subfragment 1, Oxygen exchange between water and ATP or phosphate. *J. Biol. Chem.* 265, 171–176.
30. Kagawa, H., and Mori, K. (1999) Molecular orbital study of the interaction between MgATP and the myosin motor domain: The highest occupied molecular orbitals indicate the reaction site of ATP hydrolysis. *J. Phys. Chem. B* 103, 7346–7352.
31. Minehardt, T. J., Marzari, N., Cooke, R., Pate, E., Kollman, P. A., and Car, R. (2002) A classical and ab initio study of the interaction of the myosin triphosphate binding domain with ATP. *Biophys. J.* 82, 660–675.

BI040002M